Desalination and Water Treatment
www.deswater.com

doi: 10.5004/dwt.2018.21863

102 (2018) 340–348
January

Studying Fenton oxidation kinetics of mixed dyes wastewater and salt effect by online spectrophotometry

Hang Xu*, Dandan Zhang, Tianlong Yu, Fengmin Wu, Hong Li

Chemical Engineering and Pharmaceutics School, Henan University of Science and Technology, Luoyang 471023, China, Tel. +86-379-64231914, emails: xhinbj@126.com (H. Xu), zddhaust@126.com (D. Zhang), ytl695140552@126.com (T. Yu), min49@126.com (F. Wu), 18437955958@163.com (H. Li)

Received 29 July 2017; Accepted 30 December 2017

ABSTRACT

Fenton oxidation is an efficient process for dye wastewater treatment. Dye processing wastewater containing both Rhodamine B (RhB) and Methylene Blue (MB) dyes was treated by Fenton oxidation and analyzed using fast online spectrophotometry. The RhB and MB molecules were simultaneously decomposed by Fenton oxidation. The best experimental conditions for highest dye degradation were found to be 10 mg/L of $FeSO_4$, 20 mg/L of H_2O_2 and a solution pH of 3. Under these conditions, nearly 100% color removal and 53% removal of chemical oxygen demand were achieved after 30 min of Fenton oxidation. It was found that the presence of NaCl had a negative effect on the color removal. Compared with the Fe^{2+}/H_2O_2 process, the Fe^{3+}/H_2O_2, Cu^{2+}/H_2O_2 and Co^{2+}/H_2O_2 Fenton-like processes showed very low dye removal efficiency. A first-order model and hyperbola model were used to describe the reaction kinetics. The hyperbola model showed outstanding performance in the description of the dye degradation with fitting coefficients of over 0.95. Based on the hyperbola model, the reactive activation energies of the RhB and MB degradation by the Fenton process were found to be 33.64 and 33.86 kJ/mol, respectively, with an Arrhenius fitting coefficient of over 0.99.

Keywords: Fenton; Oxidation; Color removal; Dye wastewater

1. Introduction

Advanced oxidization processes (AOPs) have excellent potential for the degradation of organic contaminants in industrial wastewater. Such oxidation mechanisms produce strong oxidants such as hydroxyl radicals (·OH) [1], which have high-activity and are non-selective when decomposing organic pollutants to CO_2, H_2O and inorganic salt within aqueous environments [2]. Depending on the generation method and the condition of the hydroxyl radicals, the types of AOPs can be divided into photochemical oxidation [3], catalytic wet air oxidation [4], ultrasound chemical oxidation [5], ozonation oxidation [6], electrochemical oxidation [7], and Fenton and Fenton-like oxidation [8,9].

Among the AOPs, the Fenton process ($Fe^{2+}/H_2O_2/H^+$) has received the greatest focus in wastewater treatment [10] because of its superior degradation efficiency, fast reaction speed and moderate investment. Dye containing wastewater is a very common refractory wastewater, which has high quantities of organic pollutants, high salinity [11] and poor biodegradability. Disastrous consequences would result if such dye containing wastewater was discharged into the environment without any treatment. Many researchers have investigated the Fenton process to treat dye wastewater and have obtained satisfactory results. For example, Karatas et al. [12] used Fenton method to treat Reactive Blue 114 dye in aqueous solutions and obtained 90% color removal. Su et al. [13] investigated Fenton oxidation to treat Reactive Black 5, Reactive Orange 16 and Reactive Blue 2 in a fluidized-bed reactor, and all three dyes were completely decomposed under the optimized experimental conditions. Sun et al. [14] also used a Fenton reagent to treat Orange G azo dye which resulted in over 90% color removal.

* Corresponding author.

1944-3994/1944-3986 © 2018 Desalination Publications. All rights reserved.

In most cases, alkali has been used to terminate the Fenton oxidation [15] as this decomposes hydrogen peroxide readily, and iron ions react with hydroxyl radicals and precipitate out as iron hydroxide ($Fe(OH)_3$). The residual solution without $Fe(OH)_3$ is used to determine the concentration of the dye. The termination of the Fenton oxidation process can generate errors. For example, the deposition of $Fe(OH)_3$ can lead to measurement errors because of flocculation and precipitation effects. The termination requires time and although this period could be minimized by a skillful researcher, experimental error is unavoidable. Online spectrophotometric technology is a fast, accurate and convenient method to monitor dye concentration without the alkali termination step. Coque et al. [16] used online spectrophotometric methods to monitor the color removal of Trypan Blue and Red Remazol. Xu et al. [17] also monitored the color removal of Reactive Brilliant Blue X-BR using online spectrophotometric methods and the Fenton oxidation process. Tunc et al. [18,19] selected Fenton's reagent to oxidize four dyes, Acid Red 66, Direct Blue 71, Acid Orange 8 and Acid Red 44, and online spectrophotometric method was used to analyze color removal. In our previous research, Reactive Red 6B was oxidized by Fenton process and online spectrophotometric method was selected as the analysis method to monitor color removal [20].

While some previous studies [15,17,20] performed by our group and others have indicated that the Fenton process successfully degraded dyes in aqueous conditions, Fenton oxidation has not been investigated for the simultaneous discoloration of two or more dyes in aqueous environments. It may well be the case that multiple dyes, in aqueous conditions, could lead to a more complex degradation process due to mutual interference. Thus, the study of dye degradation kinetics of multiple dyes would be more difficult than that of a single dye.

In this paper, two non-azo dyes widely used in the printing industry, Rhodamine B (RhB) and Methylene Blue (MB), were selected as the target contaminants in an aqueous solution. The dyes were simultaneously treated by Fenton oxidation process and monitored using online spectrophotometry to detect the changes in the wastewater. It is believed that the initial Fe^{2+} dosage, the initial hydrogen peroxide (H_2O_2) dosage, the pH value and the system temperature have an effect on the dyes' degradation. In real wastewaters, sodium chloride (NaCl) is a common salt [21] and has a detrimental impact on wastewater treatment, especially in AOPs [22]. Herein, different concentrations of NaCl were used to interfere with the dye degradation by Fenton oxidation. In many reports about Fenton oxidation kinetics, pseudo-first-order kinetics was observed [23,24]. Behnajady et al. [25] also used a pseudo-hyperbolic kinetics model to describe the Fenton process for C.I. Acid Yellow 23 degradation and the results exhibited that the hyperbola model kinetics was more suitable than pseudo-first-order kinetics. In other research papers, the hyperbolic model kinetics was also shown to be better than first-order model in dye degradation performance. In this study, both first-order kinetics and hyperbolic model kinetics were therefore investigated.

2. Experimental

2.1. Reagents

Analytical grade RhB and MB dyes were purchased from Aladdin (e-store) and the chemical structures of RhB and MB were shown in Table 1. Ferrous sulfate ($FeSO_4{\cdot}7H_2O$), copper sulfate pentahydrate ($CuSO_4{\cdot}5H_2O$), ferric sulfate ($Fe_2(SO_4)_3$), cobaltous nitrate hexahydrate ($Co(NO)_2{\cdot}6H_2O$), hydrogen peroxide (H_2O_2), sulfuric acid (H_2SO_4), sodium hydroxide (NaOH) and sodium chloride (NaCl) were analytically pure and purchased from Aladdin (e-store).

2.2. Online spectrophotometric system

The online reaction and spectrophotometric analysis system are shown in Fig. 1. This system consists of a reaction container, a digital display thermostat magnetic stirrer (85-2, Shanghai instrument manufacturer), a digital pH meter (PHS-3C-01 experimental pH meter, Hangzhou instrument

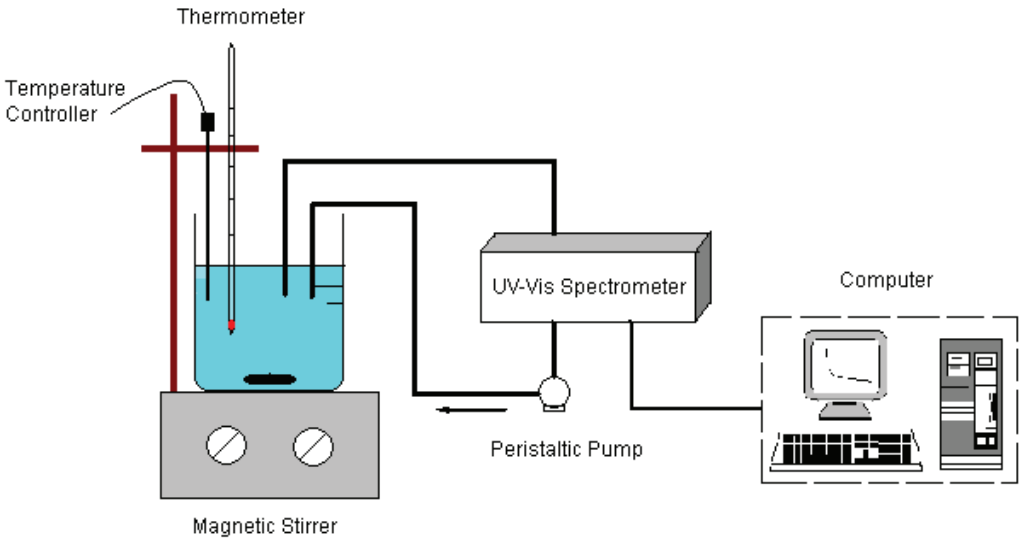

Fig. 1. Online spectrophotometric system.

limited corporation), a UV–Vis spectrophotometer (SP-756PC, Shanghai spectrometric instrument manufacturer), a peristaltic pump (HL-1D, Beijing instrument manufacturer) and computer. A plastic hose with an inner diameter of 2 mm connects the reaction solution with the flowing cell cuvette within the spectrophotometer with the solution pumped by the peristaltic pump. The return liquid is sent back to a beaker to form the cycle. UV–Vis spectrophotometry was used to monitor the color change in the flowing cell cuvette at certain times.

2.3. Fenton procedure

A 100 ml aqueous wastewater solution containing 4 mg/L RhB and 4 mg/L MB was stirred in a beaker to obtain a uniform solution. The pH value was adjusted using HCl and the reaction solution was maintained at a certain temperature. Ferrous ions were added into the system first, and then H_2O_2, as the source of active radicals, was added separately to reduce experimental error. The absorbance of RhB and MB over the range of 455–745 nm was monitored by UV–Vis spectrometry and recorded by the computer every 1 min during the 30 min experiment.

3. Results and discussion

3.1. Degradation spectra of mixed dyes

Fig. 2 shows the UV–Vis spectra of mixed RhB and MB during Fenton oxidation from 0 to 10 min. It can be clearly observed that the maximum absorption peaks of RhB and MB are at 556 and 663 nm, respectively. During the Fenton reaction, the maximum absorption peaks of RhB and MB decrease quickly. After 10 min, the removal of RhB was above 80% and removal of MB was above 90%. Fenton process is non-selective in the treatment of RhB and MB, which agrees with the hydroxyl radical oxidation mechanism. The chemical structures of RhB and MB were decomposed by hydroxyl radicals to a similar extent. In the following reactions, the absorbance values of RhB at 556 nm and MB at 663 nm were acquired from the degradation spectra at different reaction times under different conditions. The relationships between the concentrations of RhB and MB and absorbance values are shown in Fig. 2. According to the two relationship equations, the concentrations of RhB and MB could be calculated. Here, the dye removal rate (R) is defined as follows:

$$R = \frac{C_0 - C_t}{C_0} \times 100\% \quad (1)$$

where C_0 represents the initial dye concentration, and C_t represents the dye concentration at t time.

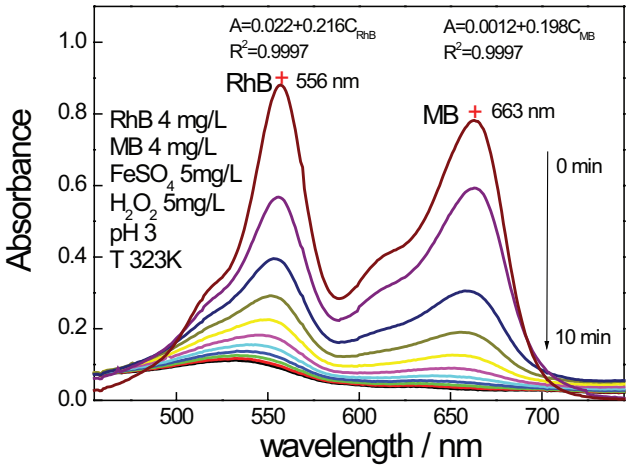

Fig. 2. UV–Vis spectra of RhB and MB during Fenton oxidation process.

3.2. Effect of Fenton reagent dosages

From Fig. 3, it can be observed that ferrous sulfate has a great influence on the removal of both dyes. At an initial dosage of 1 mg/L $FeSO_4$, about 43% and 38% of MB and RhB were removed, respectively. When the initial dosage of $FeSO_4$ was increased to 5 mg/L, the degradations of MB and RhB increased to 95% and 85%, respectively. A further increment in $FeSO_4$ dosage accelerated the reaction rate but failed to enhance the discoloration. When the $FeSO_4$ dosage was about 40 mg/L, the color removal decreased and the degradation rate was 90% and 80% for MB and RhB, respectively. For example, the removal of MB and RhB after 15 min of Fenton oxidation was about 82% and 70%, respectively, at an initial dosage of 5 mg/L $FeSO_4$. It can be seen in Fig. 3 that the optimal $FeSO_4$ initial dosage was 20 mg/L for MB and 10 mg/L for RhB.

It is known that ferrous ion acts as a promoter [26], as seen in Fig. 3. Intricate chain reactions are triggered when the ferrous ion reacts with H_2O_2. The hydroxyl radical is then generated and at the same time, ferrous ion loses one electron to form ferric ion. The partial ferric ion further consumes H_2O_2 to produce a hydroperoxyl radical and ferrous ion to exhibit a ferrous ion cycle (Eqs. (2) and (3)). Some ferric ions react with the hydroperoxyl radical to produce oxygen and ferrous ions (Eq. (4)). At the same time, self-consumption between hydroxyl or hydroperoxyl radicals and ferrous ions also undermines the primary reaction (Eq. (2)), leading to lower removal rate (Eqs. (5) and (6)) [27]. Hence, excessive $FeSO_4$ dosages are detrimental for the degradation rate.

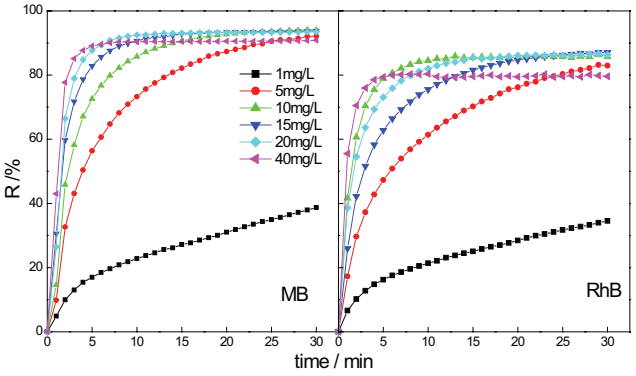

Fig. 3. The removal of MB and RhB at different $FeSO_4$ initial dosages (5 mg/L H_2O_2, pH = 3 and T = 298 K).

$$Fe^{2+} + H_2O_2 \rightarrow Fe^{3+} + OH^- + \cdot OH \quad (2)$$

$$Fe^{3+} + H_2O_2 \rightarrow Fe^{2+} + H^+ + \cdot O_2H \quad (3)$$

$$Fe^{3+} + \cdot O_2H \rightarrow Fe^{2+} + O_2\ H^+ \quad (4)$$

$$Fe^{2+} + \cdot OH \rightarrow Fe^{3+} + OH^- \quad (5)$$

$$Fe^{2+} + \cdot O_2H \rightarrow Fe^{3+} + HO_2^- \quad (6)$$

From Fig. 3, it can be seen that 15 mg/L $FeSO_4$ dosage was less effective than 10 and 20 mg/L in the RhB degradation process. Although the hydroxyl radical is a non-selective oxidizing agent, its effect on structural stability of contaminants is different. In 15 mg/L $FeSO_4$ dosage condition, more hydroxyl radicals attacked MB than RhB. In 20 mg/L $FeSO_4$ dosage condition, more hydroxyl radicals were produced. After the majority of MB had been decomposed by hydroxyl radicals, the excess hydroxyl radicals decomposed RhB to improve RhB removal. Moreover, a large amount of by-products was produced after MB and RhB decomposition. There is competition between MB, RhB and by-products for reacting with hydroxyl radicals. It is likely that at the 15 mg/L $FeSO_4$ dosage condition, more hydroxyl radicals reacted with MB and by-products than with RhB. Compared with a single pollutant, it was more difficult to study the degradation of the two mixed pollutants in the same Fenton process.

From Fig. 4, it can be observed that the discoloration rates of MB and RhB kept increasing when the H_2O_2 dosage ranged from 1 to 20 mg/L. The desired removal of 98% MB and 95% RhB can be reached after 30 min of Fenton oxidation. However, a slight decrease was observed when the H_2O_2 concentration was 50 mg/L, and this decreasing trend continued until a concentration of 100 mg/L. This phenomenon indicated that excessive H_2O_2 is not only a waste but also detrimental to the removal process. It was found that the best H_2O_2 initial dosage was 20 mg/L for the treatment of MB and RhB.

Another significant factor in the Fenton process is the hydroxyl radical consumption. In this case, a hydroxyl radical (2.8 eV) reacts with excess hydrogen peroxide to produce oxygen and water (Eqs. (7) and (8)) [28,29]. This further confirms that excessive H_2O_2 can be a disadvantage for the Fenton oxidation.

$$H_2O_2 + \cdot OH \rightarrow H_2O + \cdot O_2H \quad (7)$$

$$\cdot OH + \cdot O_2H \rightarrow O_2 + H_2O \quad (8)$$

3.3. Effect of media pH value

A series of solutions with different pH values (2, 3, 4, 5 and 7) was prepared for investigating the pH effect on discoloration rate of MB and RhB, and the results are shown in Fig. 5. At pH 2, the removal of MB and RhB was only 65% and 50%, respectively, because hydroxyl radicals reacted with the large amount of H^+ ions in a strongly acidic solution (Eq. (9)). Several researchers have suggested that the ideal pH value for the Fenton process ranges from 3 to 4, which has been confirmed by our results. In Fig. 5, it can be seen that the discoloration reached a maximum at pH 3 and decreased at pH 4. The lowest dye removal was observed at pH 7, which can be attributed to the hydrolysis of ferrous ion and the stabilization of H_2O_2. These results show that the Fenton oxidation has the best activity in a weakly acidic environment at pH 3, with 92% removal of MB and 83% removal of RhB observed after 30 min of Fenton process.

$$\cdot OH + H^+ + e^- \rightarrow H_2O \quad (9)$$

3.4. Effect of reaction temperature

As shown in Fig. 6, the effect of reaction temperature on the degradation was investigated, and temperatures from 287 to 323 K were selected. The lowest activity was observed at 287 K with only about 64% removal of MB and 57% of RhB. Higher temperatures showed higher degradation rates, which can be ascribed to the greater energy associated with molecule collision with increasing temperature. When the solution was at the highest temperature of 323 K, the two

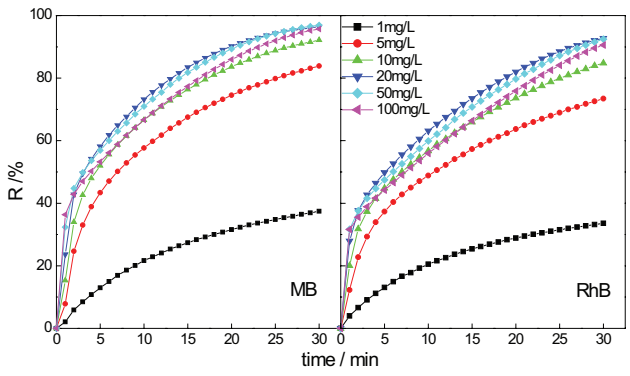

Fig. 4. The removal of MB and RhB at different H_2O_2 contents (5 mg/L $FeSO_4$, pH = 3 and T = 298 K).

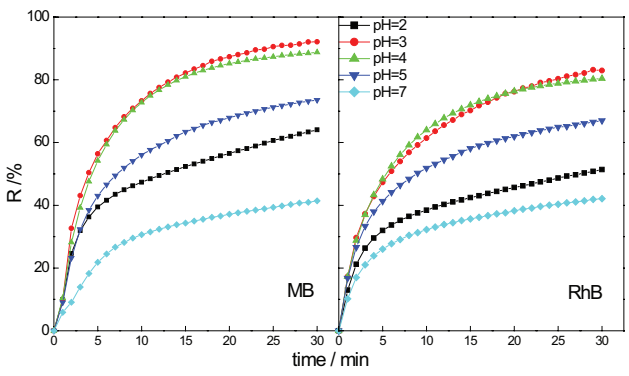

Fig. 5. The removal of MB and RhB at different pH values (5 mg/L $FeSO_4$, 5 mg/L H_2O_2 and T = 298 K).

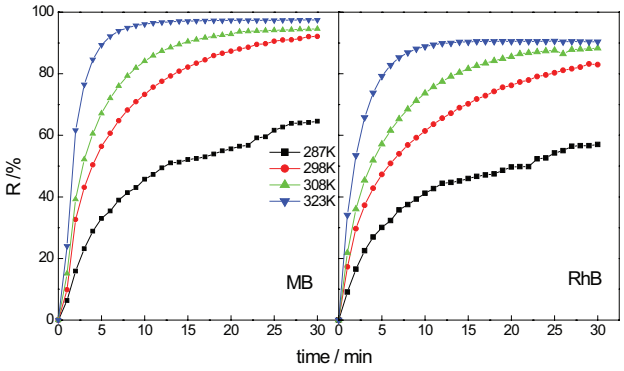

Fig. 6. The removal of MB and RhB at different temperatures (5 mg/L $FeSO_4$, 5 mg/L H_2O_2 and pH = 3).

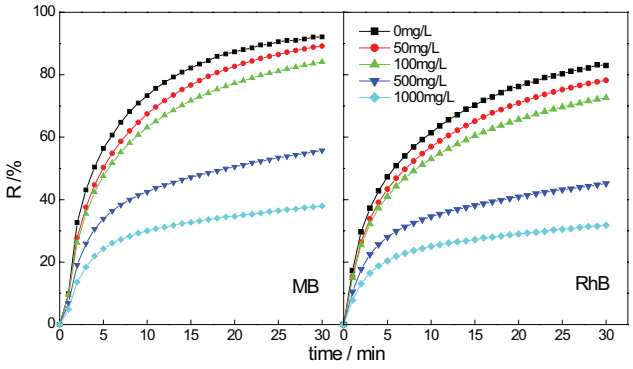

Fig. 7. The removal of MB and RhB at different NaCl concentrations (5 mg/L $FeSO_4$, 5 mg/L H_2O_2, pH = 3 and 298 K).

dye removal rates both reached about 90% in 5 min. High temperature can also accelerate the H_2O_2 decomposition and produce more hydroxyl radicals in order to increase discoloration performance.

3.5. Effect of NaCl concentration

Normally, the effluent that comes out of printing houses contains high concentration of salts which are used as the dyeing auxiliaries, where NaCl is typically the salt with the highest concentration [30]. The effect of different NaCl contents on the mixed dyes degradation is illustrated in Fig. 7. The discoloration rate decreased by 10% when the NaCl content ranged from 0 to 100 mg/L. When the NaCl content was increased to 500 mg/L, a significant decrease in dye removal was observed. Moreover, 38% decolorization rate of MB and 32% of RhB were observed after 30 min when the NaCl concentration was 1,000 mg/L. Therefore, NaCl had a significant negative impact on the Fenton oxidation process, likely due to the scavenging ability of chloride ions:

$$Cl^- + \cdot OH \rightarrow ClHO^-_{\cdot} \quad (10)$$

$$ClHO^-_{\cdot} + H^+ \rightarrow H_2O + Cl\cdot \quad (11)$$

The reaction time was also prolonged to 390 min in order to investigate the effect of degradation time at 1,000 mg/L NaCl. It can be seen in Fig. 8 that the ultimate discoloration rates of the two dyes were 35% for MB and 30% for RhB after 30 min of Fenton oxidation. When the reaction time was further increased, MB and RhB still showed acceptable removal rates before 330 min. In the last interval of 60 min the Fenton reaction approached completion. The final removal rate of MB was about 64% and that of RhB was about 52%. Therefore, even prolonging the reaction time failed to promote the dye removal efficiency in the presence of 1,000 mg/L NaCl.

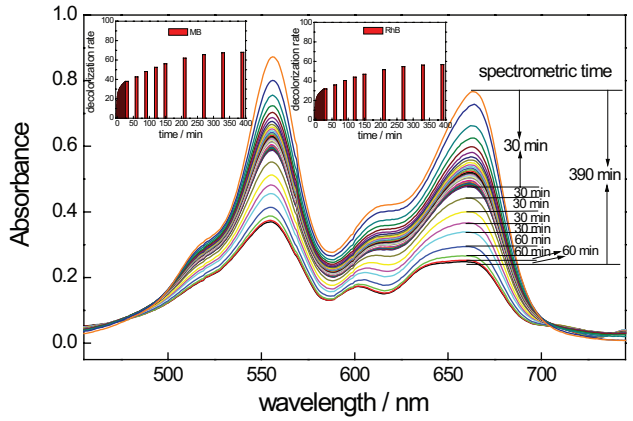

Fig. 8. The decolorization in extended experiment time (5 mg/L $FeSO_4$, 5 mg/L H_2O_2, pH = 3 and 1,000 mg/L NaCl).

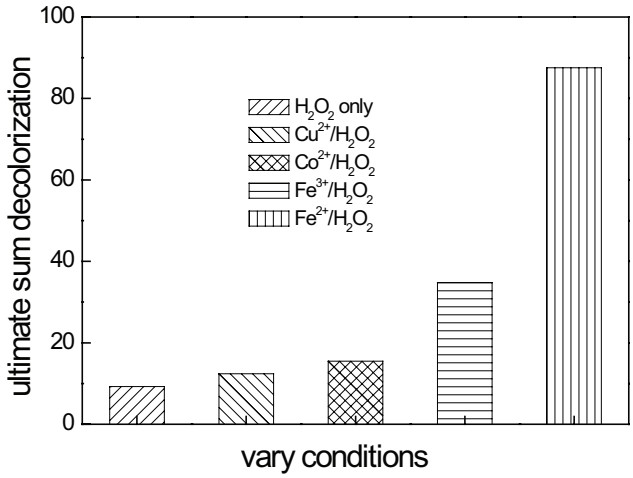

Fig. 9. The decolorization of dyes with different metal salts (5 mg/L $FeSO_4$, 8.21 mg/L $CuSO_4$, 9.57 mg/L $Co(NO_3)_2$, 6.26 mg/L $Fe_2(SO_4)_3$, 5 mg/L H_2O_2 and pH = 3).

3.6. Comparison of different metals for a Fenton-like process

In order to investigate the choice of metal ion catalyst in the Fenton-like processes, the same molar dosages of Fe^{2+}, Cu^{2+}, Fe^{3+} and Co^{2+} with H_2O_2 were used to degrade the two dyes simultaneously in solution. As shown in Fig. 9, pure H_2O_2 showed the lowest degradation performance with 9% discoloration. Then, Cu^{2+}, Co^{2+}, Fe^{3+} and Fe^{2+} ions followed an incremental order in catalytic ability. Specifically,

the Cu^{2+}/H_2O_2 process had a 12% sum discoloration rate which was similar to the Co^{2+}/H_2O_2 performance with a 16% sum discoloration rate. The Fe^{3+}/H_2O_2 process displayed a better treatment rate with 35% sum removal. Clearly, these processes need external assistance to improve the degradation efficiency. The Fe^{2+}/H_2O_2 process exhibited the best degradation performance with 88% total dye removal.

Table 1
The chemical information of Rhodamine B and Methylene Blue

Name and formula	Chemical structure	λ_{max}	M
Rhodamine B (RhB) $C_{28}H_{31}ClN_2O_3$	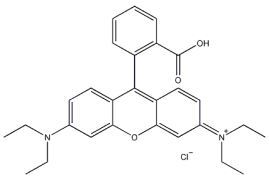	556	479.01
Methylene Blue (MB) $C_{16}H_{18}ClN_3S$	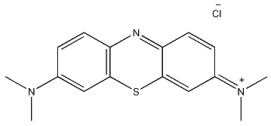	663	319.85

3.7. Kinetics analysis

The mixed solution containing both RhB and MB was successfully discolored and the process kinetics was analyzed by a first-order model and a hyperbola model (B-M-G model) which has been proposed by Behnajady et al. [25] in several publications [18–20]. The detailed formulae for the first-order model and B-M-G model are shown in Eqs. (12) and (13).

$$\frac{dC}{dt} = k_{ap}t \tag{12}$$

$$\frac{C_t}{C_0} = 1 - \frac{t}{m + bt} \tag{13}$$

where t is the reaction time; C is the dye concentration; C_0 represents the dye initial concentration; C_t represents the dye concentration at time t; k_{ap} is the reaction rate constant; and m and b are two characterization constants.

Table 2
Degradation kinetics data of RhB

$FeSO_4$ (mg/L)	H_2O_2 (mg/L)	pH	T (K)	NaCl (mg/L)	First-order model		B-M-G model		
					k (min^{-1})	R^2	m (min)	b	R^2
1	5	3	298	0	0.011	0.971	12.86	3.03	0.988
5	5	3	298	0	0.053	0.979	4.71	1.10	0.999
10	5	3	298	0	0.056	0.925	2.77	1.04	0.999
15	5	3	298	0	0.044	0.811	1.49	1.08	0.999
20	5	3	298	0	0.036	0.700	1.22	1.09	0.987
40	5	3	298	0	0.017	0.483	0.75	1.12	0.932
4	1	3	298	0	0.012	0.971	23.72	2.42	0.998
4	5	3	298	0	0.038	0.984	6.83	1.25	0.997
4	10	3	298	0	0.054	0.993	3.95	1.23	0.984
4	20	3	298	0	0.078	0.995	2.75	1.18	0.951
4	50	3	298	0	0.074	0.992	2.39	1.26	0.900
4	100	3	298	0	0.067	0.989	2.42	1.34	0.859
5	5	2	298	0	0.017	0.924	5.83	1.91	0.997
5	5	3	298	0	0.053	0.979	4.713	1.10	0.999
5	5	4	298	0	0.048	0.950	4.75	1.08	0.999
5	5	5	298	0	0.030	0.937	4.65	1.41	0.998
5	5	7	298	0	0.013	0.909	7.58	2.25	0.999
5	5	3	287	0	0.025	0.955	9.34	1.50	0.999
5	5	3	298	0	0.053	0.979	4.71	1.10	0.999
5	5	3	308	0	0.064	0.949	3.59	0.99	0.999
5	5	3	323	0	0.053	0.761	1.84	0.98	0.989
5	5	3	298	0	0.053	0.979	4.71	1.09	0.999
5	5	3	298	50	0.045	0.975	5.38	1.16	0.999
5	5	3	298	100	0.037	0.966	5.45	1.27	0.999
5	5	3	298	500	0.015	0.910	7.39	2.08	0.999
5	5	3	298	1,000	0.009	0.881	9.66	2.91	0.999

Table 3
Degradation kinetics data of MB

$FeSO_4$ (mg/L)	H_2O_2 (mg/L)	pH	T (K)	NaCl (mg/L)	First-order model		B-M-G model		
					k (min^{-1})	R^2	m (min)	b	R^2
1	5	3	298	0	0.014	0.978	17.49	2.33	0.996
5	5	3	298	0	0.080	0.978	8.21	0.57	0.957
10	5	3	298	0	0.082	0.918	5.17	0.69	0.945
15	5	3	298	0	0.065	0.812	2.06	0.92	0.967
20	5	3	298	0	0.055	0.710	2.37	0.88	0.923
40	5	3	298	0	0.034	0.577	1.06	1.01	0.915
4	1	3	298	0	0.015	0.978	43.46	0.44	0.984
4	5	3	298	0	0.055	0.989	10.59	0.64	0.967
4	10	3	298	0	0.078	0.995	5.23	0.91	0.989
4	20	3	298	0	0.103	0.997	3.20	0.98	0.993
4	50	3	298	0	0.105	0.995	2.24	1.08	0.959
4	100	3	298	0	0.092	0.992	1.99	1.17	0.898
5	5	2	298	0	0.026	0.941	7.89	1.26	0.976
5	5	3	298	0	0.080	0.979	8.21	0.57	0.957
5	5	4	298	0	0.068	0.955	7.95	0.64	0.974
5	5	5	298	0	0.038	0.950	9.11	0.88	0.979
5	5	7	298	0	0.015	0.923	15.62	1.84	0.995
5	5	3	287	0	0.030	0.962	13.55	0.89	0.984
5	5	3	298	0	0.080	0.979	8.21	0.57	0.957
5	5	3	308	0	0.091	0.943	5.21	0.72	0.969
5	5	3	323	0	0.091	0.798	2.79	0.80	0.935
5	5	3	298	0	0.080	0.979	8.21	0.57	0.957
5	5	3	298	50	0.069	0.983	8.68	0.63	0.971
5	5	3	298	100	0.055	0.974	8.67	0.73	0.975
5	5	3	298	500	0.021	0.920	11.71	1.18	0.970
5	5	3	298	1,000	0.012	0.878	16.37	1.74	0.967

The integral form of Eq. (12) is as follows:

$$\ln\frac{C_0}{C_t} = k_{ap}t \tag{14}$$

Eq. (13) can be transformed to Eq. (15) where $1/t$ is in direct proportion to $C_0/(C_0 - C_i)$.

$$\frac{1}{t}m + b = \frac{C_0}{C_0 - C_i} \tag{15}$$

The constant m reverses with the reaction rate and constant b can be a reference to determine the final degradation level. A b value that ranges from 0 to 1 means a completed degradation but also implies that there is still a certain amount of dye remaining. The experimental data and results of kinetics analysis are shown in Tables 2 and 3. Based on the results, it is seen that the hyperbola B-M-G model represented the degradation of both dyes better as most of the fitting coefficients were over 0.95. The fitting coefficients of first-order fluctuated between 0.90 and 0.99 and in some cases fell below 0.90.

The activation energy (E_a) of this mixed degradation can be calculated through Eq. (16):

$$\ln\frac{1}{m} = \frac{-E_a}{RT} + \ln A \tag{16}$$

where m is the hyperbola B-M-G model constant (representing the velocity of the process), A is the Arrhenius constant, T is the solution temperature in K, E_a is activation energy and R is the ideal gas constant. According to the data from Tables 2 and 3, there is a perfect linear relationship between $1/T$ and $\ln(1/m)$ with a fitting coefficient of over 0.99 (Fig. 10). The reaction activation energy of RhB and MB degradation by Fenton process was found to be 33.64 and 33.86 kJ/mol, respectively. Such a low energy barrier indicated that the reaction can be easily initiated without large external heat supply.

3.8. By-products analysis

Fig. 11 shows the UV–Vis spectra of the RhB and MB mixture after the Fenton oxidation from 0 to 30 min. Chemical oxygen demand (COD) and color removal are also shown in Fig. 11. It can be seen clearly that the absorbance of mixed

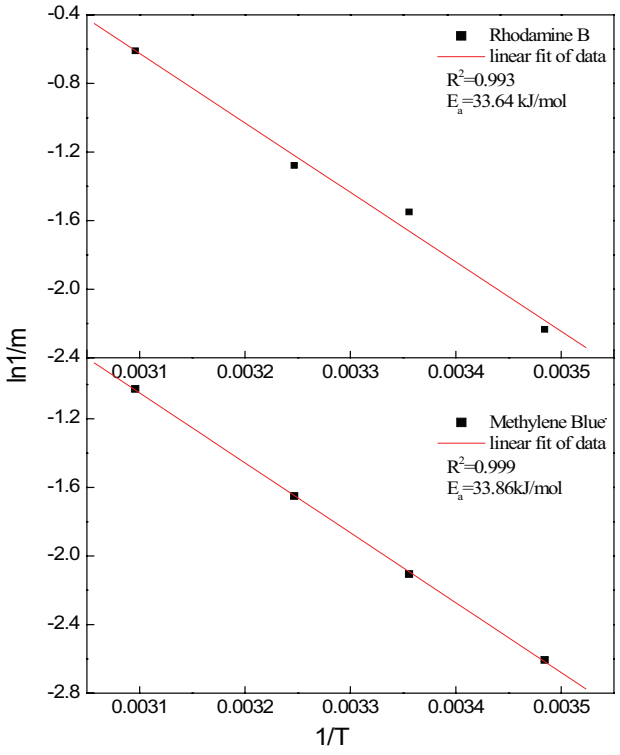

Fig. 10. Linear fitting between 1/*T* and ln(1/*m*) for thermodynamic calculation.

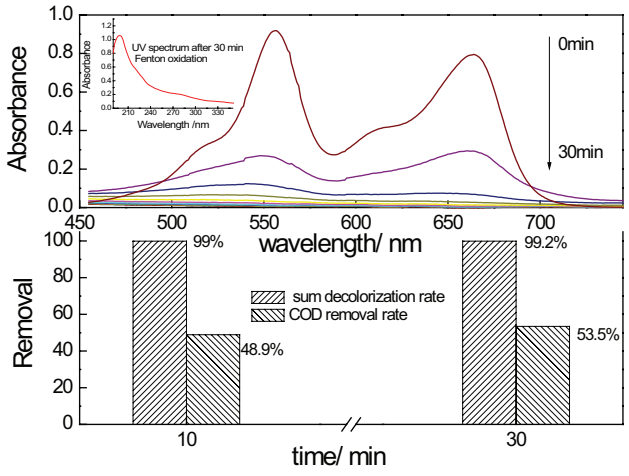

Fig. 11. The decolorization at optimum conditions (10 mg/L $FeSO_4$, 20 mg/L H_2O_2, pH = 3 and 298 K).

RhB and MB disappeared after 30 min of oxidation. However, there was a large absorbance in the ultraviolet region after 30 min. A large number of intermediate products were produced by the Fenton process after 30 min. Although color removal was close to 100%, COD removal amounts at 10 and 30 min of the Fenton process were about 48.9% and 53.5%, respectively, which showed incomplete mineralization. Even though over half of the COD was successfully removed after 30 min, there was not enough time to thoroughly mineralize this mixed RhB and MB wastewater.

4. Conclusions

Online spectrophotometry was used to monitor the absorbance of RhB and MB dyes in the Fenton process. The best experimental conditions were found to be 10 mg/L of $FeSO_4$, 20 mg/L of H_2O_2 and solution pH of 3. Under these conditions, nearly 100% color removal and 53% COD removal was achieved after 30 min of Fenton oxidation. High concentration of NaCl was found to lower the Fenton efficiency, which is attributed to hydroxyl radicals being scavenged by chloride ions. The first-order model and hyperbola B-M-G model were used to describe the degradation reaction kinetics. The B-M-G model showed outstanding performance in the description of the dyes degradation as most of the fitting coefficients were over 0.95. Based on the B-M-G model, the reaction activation energies of the RhB and MB degradation by the Fenton process were 33.64 and 33.86 kJ/mol, respectively.

Acknowledgments

This work is supported by the Nature Science Foundation of Henan Province (No: 162300410083), National Nature Science Foundation of China (No: 21006057) and Youth Teacher Support Program of Henan Provincial University (No: 2014GGJS-055).

References

[1] M. Cheng, G. Zeng, D. Huang, C. Lai, P. Xu, C. Zhang, Y. Liu, Hydroxyl radicals based advanced oxidation processes (AOPs) for remediation of soils contaminated with organic compounds: a review, Chem. Eng. J., 284 (2016) 582–598.
[2] O.U. Inmaculada, M.C. Anuska, L.R. Juan, E. Santiago, Advanced technologies for water treatment and reuse, AIChE J., 61 (2015) 3146–3158.
[3] D.X.M. Vargas, J.R.D. Rosa, C.J.L. Ortiz, A.H. Ramirez, G.A.F. Escamilla, C.D. Garcia, Photocatalytic degradation of trichloroethylene in a continuous annular reactor using Cu-doped TiO_2 catalysts by sol-gel synthesis, Appl. Catal., B, 179 (2015) 249–261.
[4] S.S. Jiang, H.P. Zhang, Y. Yan, Catalytic wet peroxide oxidation of phenol wastewater over a novel Cu-ZSM-5 membrane catalyst, Catal. Commun., 71 (2015) 28–31.
[5] S.Y. Jia, H.J. Han, H.F. Zhuang, P. Xu, B.L. Hou, Advanced treatment of biologically pretreated coal gasification wastewater by a novel integration of catalytic ultrasound oxidation and membrane bioreactor, Bioresour. Technol., 189 (2015) 426–429.
[6] S. Byun, J.S. Taurozzi, V.V. Tarabara, Ozonation as a pretreatment for nanofiltration: effect of oxidation pathway on the permeate flux, Sep. Purif. Technol., 149 (2015) 174–182.
[7] L.Z. Wang, B. Wu, P. Li, B. Zhang, N. Balasubramanian, Y.M. Zhao, Kinetics for electro-oxidation of organic pollutants by using a packed-bed electrode reactor (PBER), Chem. Eng. J., 284 (2016) 240–246.
[8] E.M. Matira, T.C. Chen, M.C. Lu, M.L.P. Dalida, Degradation of dimethyl sulfoxide through fluidized-bed Fenton process, J. Hazard. Mater., 300 (2015) 218–226.
[9] X.F. Wang, Y. Pan, Z.R. Zhu, J.L. Wu, Efficient degradation of Rhodamine B using Fe-based metallic glass catalyst by Fenton-like process, Chemosphere, 117 (2014) 638–643.
[10] A. Azizi, M.R.A. Moghaddam, R. Maknoon, E. Kowsari, Comparison of three combined sequencing batch reactor followed by enhanced Fenton process for an azo dye degradation: bio-decolorization kinetics study, J. Hazard. Mater., 299 (2015) 343–350.
[11] X.A. Ning, J.Y. Wang, R.J. Li, W.B. Wen, C.M. Chen, Y.J. Wang, Z.Y. Yang, J.Y. Liu, Fate of volatile aromatic hydrocarbons in

the wastewater from six textile dyeing wastewater treatment plants, Chemosphere, 136 (2015) 50–55.
[12] M. Karatas, Y.A. Argun, M.E. Argun, Decolorization of antraquinonic dye, Reactive Blue 114 from synthetic wastewater by Fenton process: kinetics and thermodynamics, J. Ind. Eng. Chem., 18 (2012) 1058–1062.
[13] C.C. Su, M.P. Asa, C. Ratanatamskul, M.C. Lu, Effect of operating parameters on decolorization and COD removal of three reactive dyes by Fenton's reagent using fluidized-bed reactor, Desalination, 278 (2011) 211–218.
[14] S.P. Sun, C.J. Li, J.H. Sun, S.H. Shi, M.H. Fan, Q. Zhou, Decolorization of an azo dye Orange G in aqueous solution by Fenton oxidation process: effect of system parameters and kinetic study, J. Hazard. Mater., 161 (2009) 1052–1057.
[15] H. Xu, M. Li, F.M. Wu, J. Zhang, Optimization of Fenton oxidation process for treatment of hexogeon industrial wastewater using response surface methodology, Desal. Wat. Treat., 55 (2015) 77–85.
[16] Y. Coque, E. Touraud, O. Thomas, On line spectrophotometric method for the monitoring of colour removal process, Dyes Pigm., 54 (2002) 17–23.
[17] H. Xu, D.X. Zhang, W.G. Xu, Monitoring of decolorization kinetics of Reactive Brilliant Blue X-BR by online spectrophotometric method in Fenton oxidation process, J. Hazard. Mater., 158 (2008) 445–453.
[18] S. Tunc, T. Gürkan, O. Duman, On-line spectrophotometric method for the determination of optimum operation parameters on the decolorization of Acid Red 66 and Direct Blue 71 from aqueous solution by Fenton process, Chem. Eng. J., 181 (2012) 431–442.
[19] S. Tunc, O. Duman, T. Gürkan, Monitoring the decolorization of Acid Orange 8 and Acid Red 44 from aqueous solution using Fenton's reagents by online spectrophotometric method: effect of operation parameters and kinetic study, Ind. Eng. Chem. Res., 52 (2013) 1414–1425.
[20] H. Xu, T.L. Yu, J.X. Wang, M. Li, Y.N. Liu, Online monitoring of Fenton-mediated reactive red 6B oxidation kinetics, Environ. Prog. Sustain. Energy, 34 (2015) 1019–1027.
[21] N. Modirshahla, M.A. Behnajady, F. Ghanbary, Decolorization and mineralization of C.I. Acid Yellow 23 by Fenton and photo-Fenton processes, Dyes Pigm., 73 (2007) 305–310.
[22] H. Xu, W.G. Xu, J.F. Wang, Degradation kinetics of azo dye Reactive Red SBE wastewater by complex ultraviolet and hydrogen peroxide process, Environ. Prog. Sustain. Energy, 30 (2011) 208–215.
[23] M.S. Yahya, N. Oturan, K.E. Kacemi, M.E. Karbane, C.T. Aravindakumar, M.A. Oturan, Oxidative degradation study on antimicrobial agent ciprofloxacin by electro-Fenton process: kinetics and oxidation products, Chemosphere, 117 (2014) 447–454.
[24] N. Masomboon, C. Ratanatamskul, M.C. Lu, Kinetics of 2,6-dimethylaniline oxidation by various Fenton processes, J. Hazard. Mater., 192 (2011) 347–353.
[25] M.A. Behnajady, N. Modirshahla, F. Ghanbary, A kinetic model for the decolorization of C.I. Acid Yellow 23 by Fenton process, J. Hazard. Mater., 148 (2007) 98–102.
[26] M.J. Liou, M.C. Lu, J.N. Chen, Oxidation of explosives by Fenton and photo-Fenton processes, Water Res., 37 (2003) 3172–3179.
[27] Z. Lin, L. Zhao, Y. Dong, Quantitative characterization of hydroxyl radical generation in a goethite-catalyzed Fenton-like reaction, Chemosphere, 141 (2015) 7–12.
[28] M.G. Alalm, A. Tawfik, S. Ookawara, Degradation of four pharmaceuticals by solar photo-Fenton process: kinetics and costs estimation, J. Environ. Chem. Eng., 3 (2015) 46–51.
[29] M. Liou, M. Lu, Catalytic degradation of nitroaromatic explosives with Fenton's reagent, J. Mol. Catal. A: Chem., 227 (2007) 155–163.
[30] L.G. Devi, C. Munikrishnappa, B.K. Nagaraj, E. Rajashekhar, Effect of chloride and sulfate ions on the advanced photo Fenton and modified photo Fenton degradation process of Alizarin Red S, J. Mol. Catal. A: Chem., 374 (2013) 125–131.